Design and analysis of a range-extended acidity detector based on a Nile red laser with tandem cuvette system

Yuwei Fang (方昱玮)[1,†], Junjie Cheng (程军杰)[2,†], Shengbo Wang (王声波)[1], Chun Gu (顾 春)[1], Gang Zou (邹 纲)[2], Hai Ming (明 海)[1], and Lixin Xu (许立新)[1,*]

[1]*Department of Optics and Optical Engineering, University of Science and Technology of China, Hefei 230026, China*
[2]*CAS Key Laboratory of Soft Matter Chemistry, Department of Polymer Science and Engineering, iChEM, University of Science and Technology of China, Hefei 230026, China*
**Corresponding author: xulixin@ustc.edu.cn*

Received February 26, 2020; accepted July 14, 2020; posted online September 17, 2020

A range-extended acidity detector based on Nile red was designed and analyzed in this work. In light of the good lasing property and solvatochromism characteristic of Nile red/ethanol solution, we have obtained laser spectra of sulfuric acid in different concentrations doped in this substrate. Moreover, to expand the acidity detection range, we proposed a tandem cuvette system containing rhodamine 6G/ethanol and Nile red/ethanol. Consequently, the detection range could be enlarged from 26 nm to 40 nm, by changing not only the wavelength peak but also by the intensity ratio of dual-wavelength laser output. In addition, by changing the detection and substrate materials, the whole detection range could be expanded, and therefore a wide range of applications in polarity and acidity detection could be implemented via this method.

Keywords: acidity detector; solvatochromism characteristic; Nile red; tandem cuvette system.
doi: 10.3788/COL202018.111402.

Since the laser was invented more than 50 years ago, its applications have been entered in plenty of fields, such as laser communication, spectroscopy, optical imaging, and biochemical detection. For many years, organic dye lasers have attracted the attention and research of many scientists because of their superiorities like simple configuration, easy operation, diversity of materials, and broadband fluorescence (FL) spectrum[1–11]. In the research of the dye laser, one of the focuses was the laser dye, which could be used as a laser gain medium. Whether an organic dye could be used as a laser gain medium depends on its energy level structure and chemical properties[12]. Recently, the most commonly used laser dyes are coumarin, xanthene (rhodamine and fluorescein), pyrromethene, etc. These laser dyes have a high intensity of FL, which is one of the essential conditions to be capable of laser gain. Among them, Nile red (NR) is a novel laser dye studied in recent years. NR, one of the most frequently studied laser dyes belong in the benzophenoxazine family, shows very a obvious solvatochromism property[13–15]. It fluoresces intensely, and in varying colors, in plenty of organic solvents and hydrophobic lipids, while the FL is completely quenched in water. In other words, the wavelength of its FL spectrum shifts bathochromically along with the increasing polarity of the solvent environment. This means that NR could act as a fluorescent hydrophobic probe[16].

The optical system used for sensing or detection has attracted a lot of attention in recent years. Xu *et al.*[17] fabricated dye-doped polymer microspheres that could monitor the slight change of environmental relative humidity by measuring the shift of the lasing mode. In light of the fact that acid rain is one of the most dangerous and widespread pollutions that causes disease and death globally, the real-time detection of trace amounts for sulfuric acid (SA) or nitric acid (NA) is of great interest and significance to a wide range of fields, like environmental science and biochemical detection. By far, the most widely used method is the acidity indicator, or colorimetric indicator, which has the advantage of being light and portable[18–20]. However, this acidity indicator is commonly susceptible to other interferents such as smoke, acetone, and gasoline, which would cause inaccurate detection results. Moreover, the principle of the acidity indicator is based on FL detection, a wide spectrum detection mechanism, which has fewer advantages than a laser-based detection system on account of the narrowband output and greater sensitivity of the latter.

Generally, studies on NR as the substrate for polarity or acidity detection have been verified for several years. Fowler and Greenspan[15] demonstrated that NR could be used as an excellent fat strain, which fluoresces only in the presence of a hydrophobic environment. Koti and Periasamy[21] illustrated that time-resolved area normalized emission spectroscopy (TRANES) analysis of the FL of NR in organized molecular assemblies of micelles, and the bilayer-polycarbonate (PC) membrane indicated two emissive species in these media. All of these works provided strong supports for the application of NR in polarity or acidity detection.

In this Letter, we designed and analyzed an acidity detector based on an NR/ethanol solution. SA, represented by nonvolatile acids, was used as the acidity environment provider. In the traditional parallel pumping structure with a single dye cuvette, we have obtained a 26 nm detection range both in 60 μg/mL and 200 μg/mL

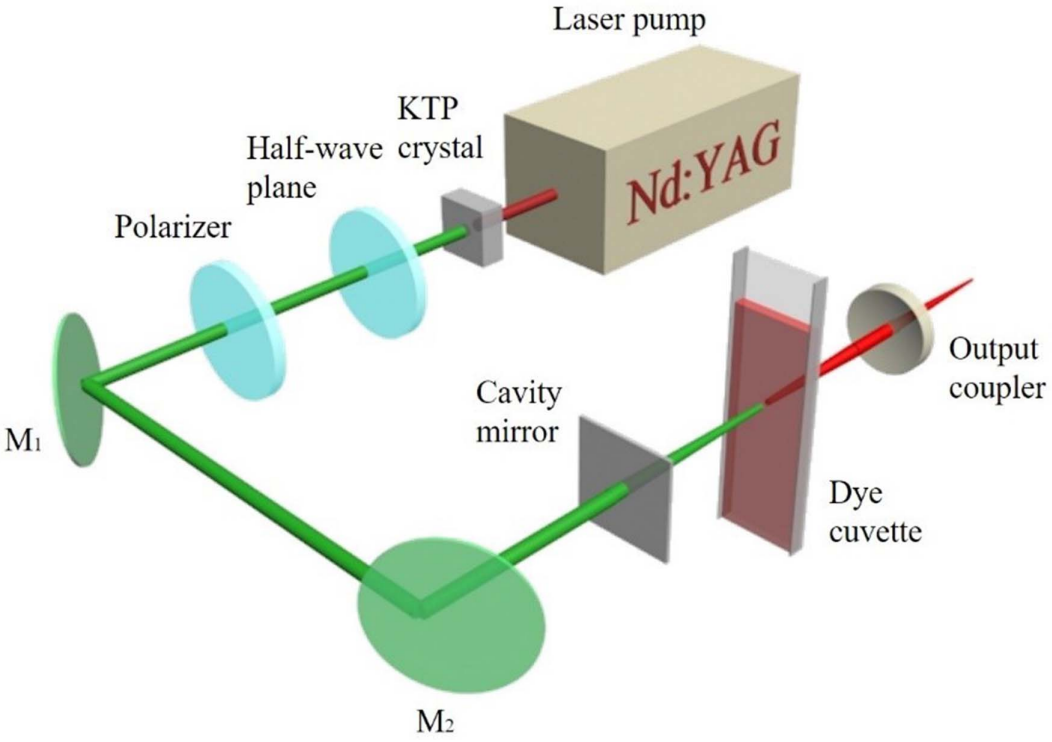

Fig. 1. Experimental setup. A potassium titanyl phosphate (KTP) crystal served as a frequency doubling crystal; the cavity mirror had high transmission (HT) at 532 nm (HT = 90%) and high reflectance (HR) in the range of 560 nm to 700 nm (HR = 90%); the output coupler had partial transmission ($R = 85\%$) from 400 nm to 700 nm.

NR/ethanol. Moreover, for the purpose of expanding the acidity detection range, we established a tandem cuvette system containing rhodamine 6G (R6G)/ethanol and NR/ethanol, which could not only be calibrated by measuring the intensity ratio of dual-wavelength laser output in low concentrations of SA doping, but also by the position of central lasing wavelength while increasing the concentration of SA. This method of an SA detection system based on NR was novel and precise. By altering the substrate material from NR to other organic laser dyes and changing SA to other detection materials like NA or acetic acid (AA), we could expand the detection range and open up new ideas for applications in acidity and polarity detection.

The experimental setup is expatiated in Fig. 1. The second harmonic generation (SHG) Q-switched neodymium-doped yttrium aluminum garnet (Nd:YAG) laser served as a laser pump, providing a laser pulse with 10 ns pulse width and 10 Hz repetition rate. A half-wave plane and a polarizer were used as modulators of input energy. M_1 and M_2 were identical plane mirrors with high reflectance at 532 nm and high transmittance at 1064 nm. The laser cavity was longitudinally pumped, which was made of a plane cavity mirror, a quartz dye cuvette, and an output coupler. The optical length of the dye cuvette was 5 mm, while the whole cavity length was set as 8 mm. A liquid laser dye was put in the dye cuvette and covered with a lid to reduce volatilization. The output laser was collected into a spectrometer (Ocean Optics, QE65000) with a resolution of 1 nm.

In our experiment, NR was selected as a laser gain medium on account of its good laser properties and sensitivity to solution polarity, which was named "solvatochromism". As Table 1 provides, the FL hypsochromically shifted from 634 nm in ethanol to 584 nm in ether, indicating its high sensitivity to polarity appreciably, which offered the possibility to polarity or acidity detection.

Since NR had good laser output properties in many organic solvents, we chose ethanol to dissolve NR in

Table 1. FL Spectra of Nile Red in Different Solvents

Solvent	Ethanol	DMF	Acetone	Chloroform	Ethyl Acetate	Ether
Relative polarity[a]	0.654	0.386	0.355	0.259	0.228	0.117
Fluorescence peak (nm)	634	616	607	602	593	584

[a]The values for relative polarity are normalized from measurements of solvent shifts of absorption spectra and were extracted from Ref. [22].

concentrations of 60 μg/mL and 200 μg/mL for preparing the detection solution systems. First of all, we carried out the pre-experiments to prove the feasibility of laser output in the NR/ethanol system. As shown in Figs. 2(a) and 2(b), the laser characteristics were substantiated initially by pumping the NR/ethanol solution at the concentration of 60 μg/mL. Figure 2(a) provides the FL and laser spectra, while the input-output curve and full width at half-maximum (FWHM) changing curve are shown in Fig. 2(b). The oscilloscope trace in Fig. 2(c) showed that the pulse width of dye laser output was in the value of 12 ns. With the increase of pumping energy, the FWHM curve of the output spectrum gradually narrowed from 46 nm to around 8 nm, and the output energy increased significantly after the pumping energy exceeded 3.1 mJ. This could help conclude that the dye laser system with the NR/ethanol solution could show good laser properties, and its energy threshold and slope efficiency were 3.1 mJ and 1.05%, respectively.

After verifying the laser properties of NR/ethanol solution in the dye laser system, SA was selected to alter the polarity of the whole environment in our experiment. With the increasing concentration of doped SA, the acidity and polarity of the whole detection environment were also increased, along with the output spectrum of the dye laser shifting bathochromically. After verifying this shifting trend, we refined the concentration of doped SA and obtained a set of output spectra. As illustrated in Fig. 2(d), SAs with different concentrations were dissolved in 60 μg/mL NR/ethanol solution, following the increasing concentrations of 10 ppm (parts per million), 20 ppm, 50 ppm, 100 ppm, 200 ppm, and 500 ppm, while 0 ppm referred to the original NR/ethanol solution with no SA. Table 2 shows the wavelength of the output laser in 60 μg/mL NR/ethanol solution corresponding to different SA concentrations. From 0 ppm to 500 ppm, the output wavelength shifted from 652.94 nm to 678.85 nm, covering about 26 nm. As the concentration of SA continued to increase (above 500 ppm), the output wavelength remained unchanged, which represented the response limit of 60 μg/mL NR/ethanol solution system to SA. Then, we changed the concentration of NR/ethanol to 200 μg/mL and obtained its output spectra in response to SA. As shown in Fig. 2(e), with the concentration of SA increased from 0 ppm to 100 ppm, the output laser shifted from 653.82 nm to 679.15 nm, also covering an about 26 nm response range. Table 3 provids the wavelength of laser output in 200 μg/mL NR/ethanol solution corresponding to different SA concentrations. While increasing the SA concentration above 100 ppm, the output wavelength could remain unchanged, which similarly represented the response limit of the 200 μg/mL NR/ethanol solution system. In order to better illustrate the influence of doped SA on the peak wavelength of the output laser, we used data in Tables 2 and 3 to plot Fig. 3. Comparing the response spectra to SA in two concentrations of NR/ethanol, the bathochromic-shift range in 60 μg/mL NR/ethanol was fairly equivalent to that in 200 μg/mL NR/ethanol, which were both nearly 26 nm. However, the SA concentrations that could be detected were up

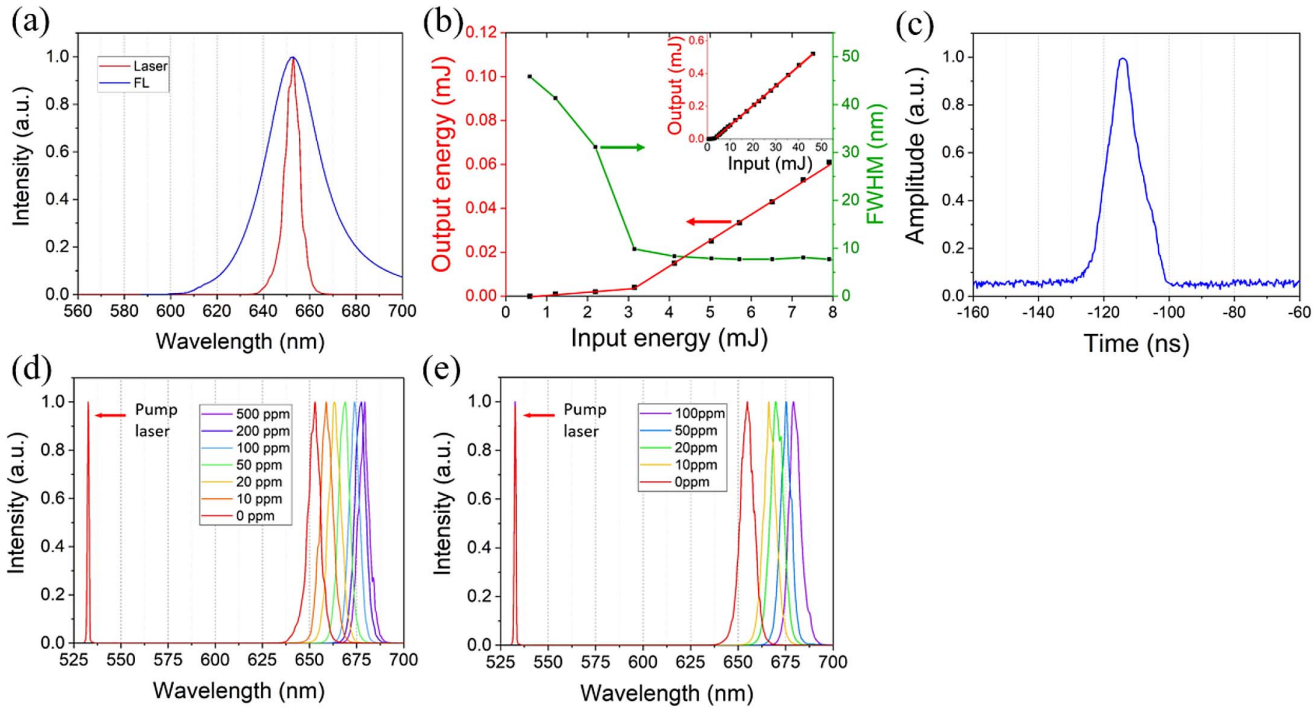

Fig. 2. (a) Laser/FL spectrum. (b) Slope efficiency curve and FWHM of the output spectrum. (c) Oscilloscope trace of output laser. (d) Spectra of output laser in 60 μg/mL NR/ethanol solution containing SA in different concentrations. (e) Spectra of output laser in 200 μg/mL NR/ethanol solution containing SA in different concentrations.

Table 2. Wavelength of Laser Output in 60 μg/mL NR/Ethanol Solution Corresponding to Different SA Concentrations

Concentration of SA (ppm)	0	10	20	50	100	200	500
Wavelength (nm)	652.94	658.88	663.07	668.93	673.83	677.48	678.85

Table 3. Wavelength of Laser Output in 200 μg/mL NR/Ethanol Solution Corresponding to Different SA Concentrations

Concentration of SA (ppm)	0	10	20	50	100	200	500
Wavelength (nm)	653.82	666.16	669.85	675.20	679.15	679.16	679.15

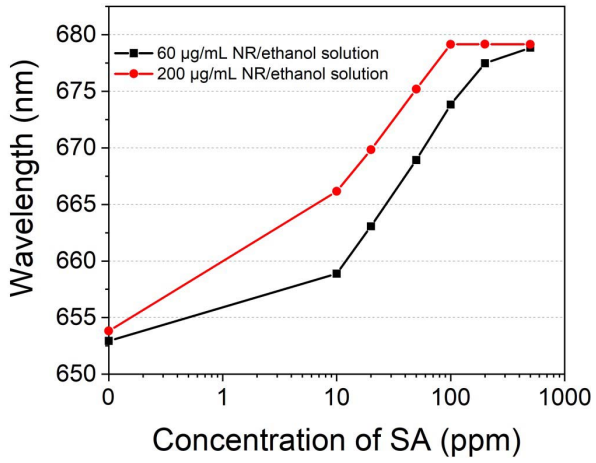

Fig. 3. Bathochromic shift of laser wavelength corresponding to different concentrations of doped SA.

to 500 ppm in the former dye solution system, while the highest detecting concentration in the later dye solution system was about 100 ppm, on account of the response limit of SA in it. Further increase of doped SA could not lead to the relative change of output laser peak. Therefore, we chose 60 μg/mL NR/ethanol solution as a detecting system to implement the acidity detection, according to the relatively large bathochromic-shift range with SA in it.

During the experiment, we observed that the acid detection range of the NR/ethanol solution system was only about 26 nm at most, which prompted us to consider whether there was a way to expand the detection range in this dye laser system. In view of this, we have implemented another structure of a dye cuvette in our experiment to expand the detection range, which was named "tandem cuvette". Figure 4(a) demonstrates the whole laser structure of the detection system, which was almost the same as the former single cuvette system in Fig. 1, while the only difference was the structure of the dye cuvette that was enlarged in the insert figure. The tandem cuvette was made of two identical quartz cuvettes and combined tightly by glue. The former cuvette was filled with R6G/ethanol at a concentration of 100 μg/mL, and the later cuvette was equipped with NR/ethanol at a concentration of 60 μg/mL. R6G was selected as one of the laser gain media on account of its good laser properties and large distance of its laser peak (at 565 nm) away from NR/ethanol laser peak.

Figures 4(b) and 4(c) provide the output spectra in this tandem cuvette system with a high/low concentration of SA in the NR/ethanol solution. As shown in Fig. 4(b), the output laser spectra shifted bathochromically from 636 nm to 676 nm, covering a nearly 40 nm range, with the concentration of SA increasing from 0 ppm to 500 ppm. This detection range was significantly extended in the tandem cuvette system compared to the former single cuvette system. This might be explained by the energy level structure and spectral overlap of these two classical dyes, NR and R6G. Shank[12] put forward the energy level structure of laser dyes in his Letter and concluded that the wide-band laser system formed by the wide-band energy level structure of dye molecules could be regarded as an equivalent four-level laser system, also named a quasi-four-level laser system. On account of the large number of different vibrational energy levels in dye molecules, the FL spectrum of dye molecules was wider. In addition, these dye molecules also had a rotational energy level structure, which finally determined the wide-band continuous emission spectrum of FL. In this tandem cuvette system, the absorption spectrum of NR/ethanol solution and the FL emission spectrum of R6G/ethanol overlapped greatly, which could lead to the result that the laser peak position would not coincide with the FL peak. The combination of multiple factors caused mode competition, which made the final NR laser output wavelength shift hypochromatically. This phenomenon was more obvious in the case of low concentration of SA doping.

In general, with the increasing concentration of SA, the wavelength of the output laser was also shifted bathochromically continuously, which meant each SA concentration should correspond to the specific output laser wavelength. While in our experiment, when considering the lower concentration of SA doping, the results might be different from what we have already known.

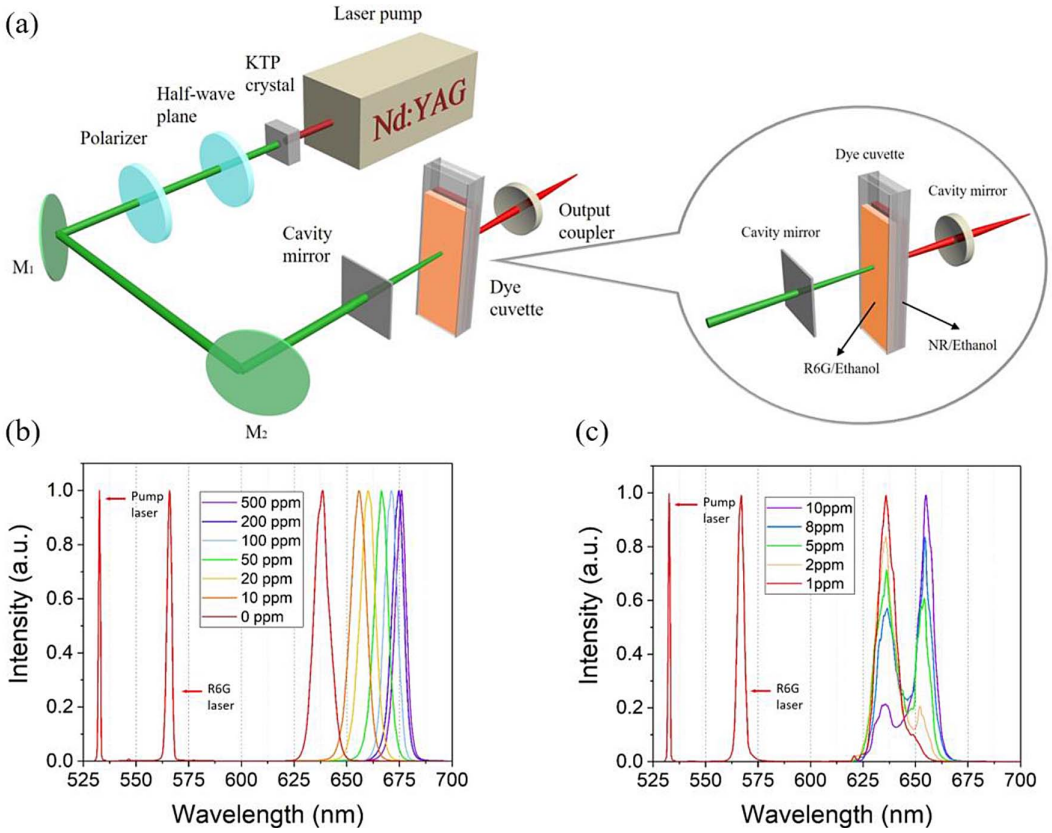

Fig. 4. (a) Tandem cuvette detection system of SA. Inset figure: details of tandem cuvette structure containing R6G/ethanol and NR/ethanol with SA. (b) Spectra of output laser in tandem cuvette system with high concentration of SA from 0 ppm to 500 ppm. The laser peak at 565 nm was in the spectrum of R6G/ethanol. (c) Spectra of output laser in tandem cuvette system with low concentration of SA from 1 ppm to 10 ppm. The laser peak at 565 nm was in the spectrum of R6G/ethanol.

As illustrated in Fig. 4(c), when we adjusted the concentration of SA from 1 ppm to 10 ppm, the output wavelength was not shifted continuously but exhibited a kind of "ratiometric laser" output characteristic. When the concentration of SA was initially 1 ppm, the central wavelength of the output laser was at 636 nm. While increasing the concentration, the laser peak at 636 nm started to decrease, while another laser peak became prominent at around 654 nm. Continuing to increase the concentration up to 10 ppm, the former laser peak almost disappeared, and the later laser peak dominated the output spectrum. This result was pioneering because we could get the quantity of SA in low concentrations by measuring the intensity ratio of the dual-wavelength laser output in this "ratiometric laser" rather than simply by the central wavelength. Table 4 provides the detection calibration of SA in different concentrations. In low concentrations (1 ppm to 10 ppm), different concentrations of SA corresponded to different intensity ratios of this dual-wavelength laser output, from normalized 0.102 to 4.630, and to the maximum of infinity. In view of this, the detection system with low to high SA concentration

Table 4. Intensity Ratio of Dual-wavelength Laser and Wavelength Position Corresponding to Different Concentration of SA in Tandem Cuvette System

Concentration of SA (ppm)	0	1	2	5	8	10	20	50	100	200	500
Intensity ratio of dual-wavelength (normalized)	0	0.102	0.143	0.851	1.390	4.630	NA	NA	NA	NA	NA
Wavelength (nm)	636.0	636.0/ 648.5	636.1/ 649.2	636.3/ 654.2	636.6/ 654.5	636.0/ 654.8	660.1	666.5	671.2	675.5	676.0

was established and calibrated in our newly proposed tandem cuvette dye laser system containing R6G/ethanol and NR/ethanol.

In conclusion, we have designed and analyzed an SA concentration detection system. NR/ethanol was chosen as the laser gain medium and substrate material. In the traditional parallel pumping structure with a single cuvette, we obtained 26 nm detection range both in 60 μg/mL NR/ethanol within the concentration of SA from 0 ppm to 500 ppm and in 200 μg/mL NR/ethanol within concentration from 0 ppm to 100 ppm. In view of the detection limit of concentration, we consequently selected the 60 μg/mL NR/ethanol as a proper detection substrate. In addition, we established a tandem cuvette system containing R6G/ethanol and original NR/ethanol as laser dye to expand the acidity detection range. In low concentrations of SA, we could calibrate by the intensity ratio of the dual-wavelength laser output. While increasing the concentration, the calibration could be realized by the position of central wavelength. This concentration detection of SA in NR/ethanol with a tandem cuvette system was precise and accurate. Meanwhile, by changing the substrate material from NR to other organic laser dyes like Congo Red (CR) or substituting the SA to other detection materials like NA or AA, we could expand the detection range in this system, and consequently more applications were likely to be found using this method in many areas.

This work was supported by the National Key Research and Development Program of China (No. 2016YFB0401901), Major Science and Technology Special Project in Anhui (No. 17030901001), National Natural Science Foundation of China (Nos. 21574120 and 21774115), Fundamental Research Funds for the Central Universities (No. WK2060200025), and Science and Technological Fund of Anhui Province for Outstanding Youth (No. 1608085J01).

†These authors contributed equally to this work.

References

1. D. Schneider, T. Rabe, T. Riedl, T. Dobbertin, M. Kröger, E. Becker, H. Johannes, W. Kowalsky, T. Weimann, J. Wang, P. Hinze, A. Gerhard, P. Stössel, and H. Vestweber, Adv. Mater. **17**, 31 (2005).
2. G. Magyar, Appl. Opt. **13**, 25 (1974).
3. S. A. Tedder, J. L. Wheeler, and P. M. Danehy, Appl. Opt. **50**, 901 (2011).
4. M. Gupta, P. Kamble, M. C. Rath, D. B. Naik, and A. K. Ray, Appl. Opt. **54**, 7013 (2015).
5. J. E. Lawler, W. A. Fitzsimmons, and L. W. Anderson, Appl. Opt. **15**, 1083 (1976).
6. F. J. Duarte, Opt. Photon. News **14**, 20 (2003).
7. T. G. Pavlopoulos, Prog. Quantum Electron. **26**, 193 (2002).
8. D. P. Dai, Y. Xia, Y. N. Yin, X. X. Yang, Y. F. Fang, X. J. Li, and J. P. Yin, Opt. Express **22**, 28645 (2014)
9. T. S. Alster and C. M. Williams, Lancet **345**, 1198 (1995).
10. D. P. Mahoney, A. A. Demissie, and R. M. Dickson, J. Phys. Chem. A **123**, 3599 (2019).
11. Q. He, F. Wang, Z. Q. Lin, C. Y. Shao, M. Wang, S. K. Wang, C. L. Yu, and L. L. Hu, Chin. Opt. Lett. **17**, 101401 (2019).
12. C. V. Shank, Rev. Mod. Phys. **47**, 649 (1975).
13. S. M. Grenci, G. R. Bird, B. W. Keelan, and A. H. Zewail, Laser Chem. **6**, 361 (1986).
14. A. P. Piechowski and G. R. Bird, Opt. Commun. **50**, 386 (1984).
15. S. D. Fowler and P. Greenspan, J. Histochem. Cytochem. **33**, 833 (1985).
16. A. Sarkar and S. Pandey, J. Chem. Eng. Data **51**, 2051 (2006).
17. W. Xu, C. X. Xu, F. F. Qin, Y. Q. Shan, Z. Zhu, and Y. Zhu, Chin. Opt. Lett. **16**, 081401 (2018).
18. S. Schutting, S. M. Borisov, and I. Klimant, Anal. Chem. **85**, 3271 (2013).
19. W. Dungchai, O. Chailapakul, and C. S. Henry, Anal. Chim. Acta **674**, 227 (2010).
20. N. C. A. Rashid, N. H. Ngajikin, A. I. Azmi, R. Arsat, S. Isaak, N. A. Cholan, and N. E. Azmi, Chin. Opt. Lett. **17**, 081701 (2019).
21. A. S. R. Koti and N. Periasamy, J. Chem. Sci. **113**, 157 (2001).
22. C. Reichardt, *Solvents and Solvent Effects in Organic Chemistry*, 3rd ed. (Wiley-VCH, 2003).